

Predictive value of posterior cranial fossa morphology in the decompression of Chiari malformation type I

A retrospective observational study

Zheng Liu, MD, Zheng Hao, MD, Si Hu, MD, Yeyu Zhao, MD, Meihua Li, MD, PhD*

Abstract

Posterior fossa decompression (PFD) is the standard procedure for the treatment of Chiari malformation type I (CMI). Although most patients have satisfactory surgical outcomes, some show no improvement or even a worsening of symptoms. Patient selection is thought to account for these different surgical outcomes. Our aim was to evaluate the predictive value of the preoperative posterior cranial fossa (PCF) morphology on the efficacy of PFD.

Data from 39 CMI patients with CMI-related symptoms who underwent occipital foramen enlargement + C-1 laminectomy + enlarged duraplasty were retrospectively collected from January 2011 to May 2018. The patients were divided into improved and unimproved groups according to the modified Chicago Chiari Outcome Scale. Demographic information and clinical history, including preoperative comorbidities and clinical manifestations, were recorded for the 2 groups and compared. PCF morphology was assessed based on 13 linear, 8 angular, 4 areal parameters and 4 ratios related to these linear and areal parameters. The data were then analyzed statistically.

Of the 39 patients with CMI, 24 showed improvement after PFD (61.5%), whereas the remaining 15 patients showed no improvement (38.5%). The preoperative symptoms lasted 1 to 240 months, with a median of 24 months. The follow-up period ranged from 2 to 82 months, with a median of 27 months. The improved and unimproved groups differed significantly with regard to upper limb numbness (OR = 10, $P = .02$) and upper limb weakness (OR = 4.86, $P = .02$). The 2 groups did not differ significantly with regard to any morphological parameters such as tonsillar descent, syrinx size.

Preoperative upper limb numbness and upper limb weakness are unfavorable factors that influence the outcome of PFD in patients with CMI. However, the morphology of PCF cannot predict the response to PFD in patients with CMI.

Abbreviations: CCOS = Chicago Chiari Outcome Scale, CMI = Chiari malformation type I, CSF = cerebrospinal fluid, ICC = intraclass correlation coefficients, ICP = intracranial pressure, ICVC = intracranial volume change, IQR = interquartile range, MR = magnetic resonance, MRI = magnetic resonance imaging, PCF = posterior cranial fossa, PFD = posterior fossa decompression, SD = standard deviation.

Keywords: Chiari malformation type I, morphology, posterior cranial fossa, posterior fossa decompression, surgical outcome

1. Introduction

At the end of the 19th century, the Austrian pathologist Hans Chiari described a malformation in which the cerebellar tonsil

herniates into the spinal canal or the medulla oblongata and fourth ventricle are displaced downward, resulting in a series of symptoms.^[1] In Chiari malformation type I (CMI), the most common type, the cerebellar tonsil descends >5 mm below the foramen magnum, without the involvement of the brain stem or fourth ventricle. It can be associated with multiple comorbidities, including syringomyelia, scoliosis, and hydrocephalus.^[2,3] The exact prevalence of CMI in the general population is unclear but, according to one report, the prevalence ranges from 0.5% to 0.9% in adults and is ~1% in children.^[4] The symptoms and signs of CMI reflect the obstruction of cerebrospinal fluid (CSF) flow, compression of the contents in the posterior cranial fossa (PCF), or spinal cord dysfunction.^[5] Surgery is the only way to treat CMI, and posterior fossa decompression (PFD) is the standard procedure. The aim of PFD is to relieve the compression of the hindbrain and cervical spinal cord induced by the abnormal anatomical structure of the PCF and thus improve CSF flow dynamics.^[6] Zhao et al assessed the data from 18 reports in the literature concerning 1242 patients with surgically treated CMI. They found that ~80% of the patients experienced relief from the symptoms and signs of CMI, whereas the remaining 20% showed no improvement after surgery.^[7] In some studies, the percentage of unfavorable outcomes after PFD was as high as 30%,^[8] although a subsequent report noted that postoperative

Editor: Devrimsel Harika Ertem.

ZL the first author.

This work was supported by the National Natural Science Foundation of China (NSFC): [grant numbers 81860225].

The authors report no conflicts of interest.

Department of Neurosurgery, the First Affiliated Hospital of Nanchang University, Nanchang, Jiangxi Province, China.

* Correspondence: Meihua Li, Department of Neurosurgery, the First Affiliated Hospital of Nanchang University, No. 17, Yongwaizheng Street, Nanchang 330019 (e-mail: limeihua2000@sina.com).

Copyright © 2019 the Author(s). Published by Wolters Kluwer Health, Inc. This is an open access article distributed under the terms of the Creative Commons Attribution-Non Commercial License 4.0 (CCBY-NC), where it is permissible to download, share, remix, transform, and buildup the work provided it is properly cited. The work cannot be used commercially without permission from the journal.

Medicine (2019) 98:19(e15533)

Received: 21 December 2018 / Received in final form: 26 February 2019 / Accepted: 9 April 2019

<http://dx.doi.org/10.1097/MD.00000000000015533>

magnetic resonance imaging (MRI) reflected adequate decompression in two-thirds of the patients with unfavorable outcomes.^[9] The high rate of unfavorable outcomes has been attributed to poor patient selection rather than to the surgical procedure.^[8–10] As people are always skeptical and prudent regarding health-related services, they will definitely not choose to have surgery if they find that PFD cannot bring them improvement.^[11] Most studies of CMI decompression efficacy have considered symptoms, syringomyelia, CSF dynamics, or PCF volumetric changes, whereas few studies have attempted to predict surgical outcome based on preoperative PCF morphology.^[5,8,12,13] Thus, in this study, we compared the morphology of the PCF in patients with and without surgical improvement. Our primary aim was to develop a method based on PCF morphology to predict which patients with CMI would respond favorably to PFD.

2. Methods

2.1. Patients

After study approval by the Institutional Review Board of the First Affiliated Hospital of Nanchang University (Nanchang, China), we retrospectively reviewed the electronic medical records of patients treated from January 2011 to May 2018 to identify individuals with CMI. The diagnostic criterion for CMI was the descent of the cerebellar tonsil >5 mm below the foramen magnum. All patients who met this criterion were older than 18 years of age and had CMI-related symptoms on admission. Only those patients whose magnetic resonance (MR) images were of sufficient quality for accurate mensuration were included in the study. Preliminary screening identified 92 consecutive cases that were eligible for further evaluation. All the included patients were treated for CMI for the first time. The surgical technique was unified occipital foramen enlargement + C-1 laminectomy + enlarged duraplasty. A small suboccipital osteoplastic craniotomy was carried out to create an occipital bone flap of 3 × 3 cm. The posterior arch of the atlas was resected 1 cm along each side of the midline. Duraplasty consisted of a Y-shaped opening of the dura to span the majority of the craniectomy area. After the adherent arachnoid was dissected and the protruding cerebellar tonsils electrocauterized with the aid of a microscope, autologous fascia or artificial dura mater, according to the surgeon's preference, was used in an enlarged duraplasty. Finally, the surgical incision was tightly sutured in layers. Patients with the following were excluded from the study:

1. accompanying trauma, rheumatic diseases, inflammation or genetic diseases;
2. congenital craniocervical junction malformations, such as basilar impression, a flat skull base, atlantoaxial fusion or dislocation;
3. tumors of the skull or tumors involving the craniocervical junction; and
4. postoperative complications, such as wound infection, intracranial bacterial infection, aseptic meningitis, or CSF leakage.

After excluding such patients, 57 individuals were included in the study. A review of the patients' medical record and structured telephone interviews were carried out to obtain information about the changes in clinical symptoms. After the loss to follow up of 18 patients (31.6%), data from 39 patients were analyzed;

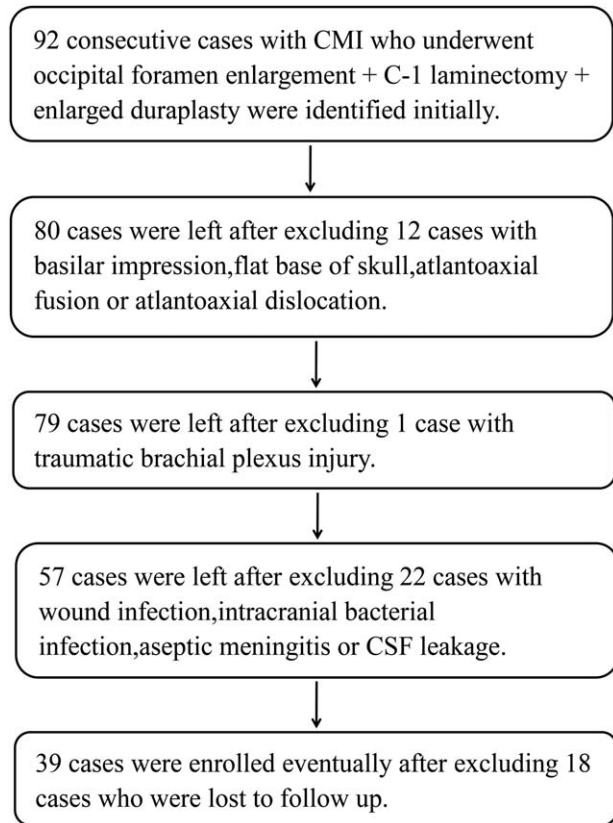


Figure 1. Flow diagram of the patient inclusion process.

the results are reported herein. A flow diagram for patient inclusion is shown in Figure 1. The characteristics of the patients, including sex, age, duration of symptoms from onset to surgery, duration from surgery to final follow up, preoperative symptoms, and presence of syringomyelia, hydrocephalus, or scoliosis, are summarized in Table 1. The age range at admission of the 29 females (74%) and 10 males (26%) was 21 to 72 years, with an average of 48.3 years. The preoperative symptoms lasted 1 to 240 months, with a median of 24 months. The follow-up period was 2 to 82 months, with a median of 27 months. Pain symptoms, including headache or limb pain, were reported by 25 patients, and non-pain symptoms, such as limb weakness or numbness, were reported by 34 patients. Syringomyelia was the most

Table 1

Demographic characteristics, preoperative symptoms, and comorbidities in patients with Chiari malformation type I.

Variable	CMI (n = 39)
Sex (male/female)	10/29
Age (years), mean ± SD	48.3 ± 9.7
Duration of symptoms (months), median (range)	24 (1–240)
Duration of follow-up (months), median (range)	27 (2–82)
Pain symptoms (%)	25 (64%)
Non-pain symptoms (%)	34 (87%)
Syringomyelia (%)	35 (89.7%)
Scoliosis (%)	6 (15.2%)
Hydrocephalus (%)	3 (8%)

CMI = Chiari malformation type I, SD = standard deviation.

common comorbidity (35 patients, 89.7%), followed by scoliosis (6 patients, 15.2%), and hydrocephalus (3 patients, 8%).

2.2. Surgical outcome reporting

Postoperative improvement was defined using a partially modified outcome scale based on the Chicago Chiari Outcome Scale (CCOS).^[14] A systematic review showed that the CCOS is the only scale with statistical validity in retrospective studies for CMI.^[15] It evaluates changes in the status of patients with CMI before and after surgery based on four subitems: pain symptoms, non-pain symptoms, function, and complications. Each subitem is assigned a score between 1 and 4, ranging from worsened to resolved. Because the assessment of function is very subjective, inter-observer consistency does not improve the discriminative power with respect to outcomes and was therefore not used as a subitem.^[16] Additionally, although the aim of the study was to determine the feasibility of preoperative MRI for predicting the efficacy of CMI decompression surgery, surgical complications may adversely affect the outcomes of decompression. To eliminate this potential source of bias, patients with surgical complications were excluded from the study. Thus, pain and non-pain symptoms were used as subitems to assess the efficacy of decompression in CMI. Patients without pain or non-pain symptoms before surgery received a score of 2. The criteria for enrollment in the improved group were:

1. a single item score ≥ 2 points; and
2. a summed pain and non-pain symptoms score ≥ 5 .

Patients who did not meet both of the above 2 conditions were included in the unimproved group.

2.3. Morphological measurement

Pre-surgical craniocervical MRI was performed with patients in a routine spinal neutral position using Siemens Skrya 3.0T scanners. All images were taken according to a standard protocol using sagittal, axial, and coronal conventional T1-weighted sequences (TR/TE, 450/9 ms). Additionally, axial T2-weighted sequences (TR/TE, 2200/105 ms) were obtained. All obtained sequences had a 3-mm slice thickness and 0.4-mm interslice gap with a 320×320 imaging matrix. The MR images of all patients were analyzed using a digital picture archiving and communication system (PACS) on a postprocessing workstation (Carestream Health, Rochester, NY). To evaluate PCF morphometry, 28 morphologic parameters including linear, angular, and areal parameters and relative ratios, were measured and calculated manually from the operator-selected, midline sagittal T1-weighted MR image data of each patient.^[17–19] The criteria for mid-sagittal image selection consisted of the visibility of at least three of four structures in a single sagittal image:

1. the genu of the corpus callosum;
2. the splenium of the corpus callosum;
3. the pituitary infundibulum; and
4. the cerebral aqueduct.^[17]

Morphological parameters were defined as follows:

2.3.1. Linear parameters.

1. Clivus: the line between the top of the dorsum sellae and the basion;
2. McRae line: the line between the basion and opisthion;

3. Supraocciput: the line between the opisthion and the internal protuberance of the occipital bone;
4. Tentorium: the line between the most posterior aspect of the corpus callosum and the internal occipital protuberance along the dural fold;
5. Tentorium–clivus line: the line between the most posterior aspect of the corpus callosum and the top of the dorsum sellae;
6. Twining line: the line from the internal occipital protuberance to the top of the dorsum sellae;
7. PCF height: the perpendicular distance from the most anterior portion of the tentorium to the McRae line;
8. PCF depth: the perpendicular distance from the top of the dorsum sellae to the extension of the McRae line;
9. Tonsillar descent: the perpendicular distance between the tip of the cerebellar tonsil and the McRae line;
10. Tonsillar width: the distance between the 2 endpoints of the cerebellar tonsil on the McRae line;
11. Fastigium height: the perpendicular distance from the fastigium of the fourth ventricle to the McRae line;
12. Pons height: the perpendicular distance from the cephalad aspect of the pons at the mid-brain junction to the McRae line.

2.3.2. Angular parameters.

1. Clival angle: formed by a line along the clivus and the extension of the McRae line;
2. Supraoccipital angle: the angle between the supraocciput and the extension of the McRae line;
3. Tentorial angle: the angle between the tentorium and the Twining line;
4. Tentorial–supraoccipital angle: the angle between the tentorium and the supraocciput;
5. Twining–supraoccipital angle: the angle between the Twining line and the supraocciput;
6. Basal angle: the angle between the line extending across the anterior cranial fossa to the top of the dorsum sellae and the line drawn along the posterior margin of the clivus;
7. Wackenheim angle: the angle between a line along the clivus and the line tangent to the posterior aspect of the odontoid process until the base of the C2 vertebra;
8. Cervicomedullary angle: the angle between the 2 lines on the ventral side of the medulla oblongata and upper cervical spinal cord.

2.3.3. Areal parameters.

1. PCF area: pentagonal area delimited by the clivus, McRae line, supraocciput, tentorium, and tentorium–clivus line;
2. PCF osseous area: quadrilateral area delimited by the clivus, McRae line, supraocciput, and Twining line;
3. Tonsillar descent area: the triangular area delimited by the 2 endpoints of the tonsil on the McRae line and the tip of the cerebellar tonsil;
4. Piston area: triangular area delimited by the endpoint of the anterior margin of the medulla oblongata on the McRae line, the endpoint of the posterior margin of the tonsil on the McRae line, and the tip of the cerebellar tonsil.

2.3.4. Relative ratios.

1. PCF height/length of the Twining line;
2. PCF depth/length of the Twining line;

3. PCF osseous area/tonsillar descent area;
4. PCF osseous area/piston area.

The maximum diameter of the cervical spinal cord syrinx on axial T2-weighted MR images was measured as well. Only syrinxes measuring at least 3 mm in their maximum dimension on axial imaging were included in the study.^[20] Intramedullary cavitations measuring <3 mm were excluded from the analysis. The maximum diameter of the syrinx was defined as the syrinx size. Figure 2 shows the measurement of the linear, angular, and areal parameters mentioned above. The linear and angular parameters were measured directly using the built-in tools of the

PACS imaging system. The tonsillar descent area and piston area were calculated according to the triangular area formula. To measure the osseous area of the PCF and the PCF area, the quadrilateral or pentagonal area was divided into 2 or 3 triangular areas, and those areas were then summed. All measurements were made independently by 2 observers (Liu, Hao) who had undergone unified standard methodological training and were blind to the symptomatic status of the patients at the time of the measurements. Inter-observer reliability was established on all images from the dataset. Two-way mixed intraclass correlation coefficients (ICCs) were computed for

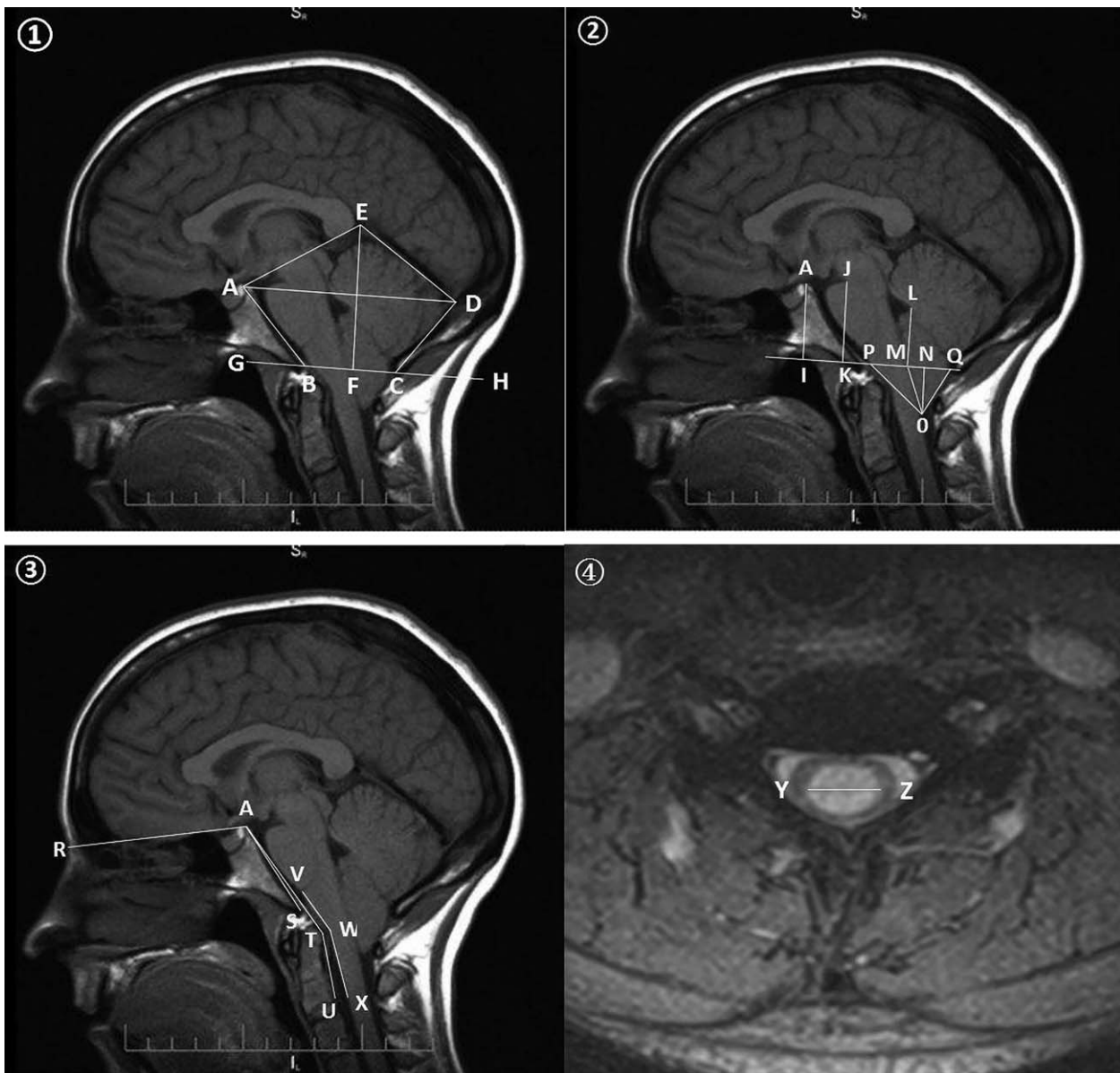


Figure 2. Sagittal T1-weighted magnetic resonance images indicating the morphologic lines, angles and areas in the posterior cranial fossa (PCF) and axial T2-weighted magnetic resonance images to determine syrinx size: ① Clivus (AB), McRae line (BC), supraocciput (CD), tentorium (DE), tentorium-clivus line (AE), Twining line (AD), PCF height (EF), clival angle (\angle ABG), supraoccipital angle (\angle DCH), tentorial angle (\angle ADE), tentorial-supraoccipital angle (\angle CDE), Twining-supraoccipital angle (\angle ADC), PCF area (the pentagonal area is delimited by A, B, C, D, and E), and PCF osseous area (quadrilateral area delimited by A, B, C, D). ② PCF depth (AI), pons height (JK), fastigium height (LM), tonsillar descent (NO), tonsillar width (MQ), tonsillar descent area (Δ MOQ), and piston area (Δ OPQ). ③ Basal angle (\angle RAS), Wackenheim angle (\angle ATU), cervicomedullary angle (\angle VWX). ④ Syrinx size (YZ).

Table 2**Inter-observer reliability for each morphologic measurement.**

Parameter	ICC value	95%CI
Clivus	0.97	0.94–0.98
McRae line	0.97	0.95–0.99
Supraocciput	0.98	0.95–0.99
Tentorium	0.98	0.93–0.99
Tentorium-clivus line	0.99	0.98–1
Twining line	0.98	0.97–0.99
PCF height	0.96	0.89–0.99
PCF deep	0.96	0.94–0.98
Pons height	0.99	0.99–1
Fastigium height	0.88	0.78–0.94
Tonsillar descent	0.97	0.94–0.98
Tonsillar width	0.95	0.90–0.97
Syrinx size	0.99	0.99–1
Clival angle	0.97	0.93–0.98
Supraoccipital angle	0.99	0.98–0.99
Tentorial angle	0.97	0.92–0.99
Tentorial-supraoccipital angle	0.98	0.95–0.99
Twining-supraoccipital angle	0.95	0.9–0.97
Basal angle	0.91	0.83–0.95
Wackenheim angle	0.98	0.95–0.99
Cervicomedullary angle	0.96	0.93–0.98
PCF area	0.96	0.87–0.99
PCF osseous area	0.90	0.8–0.94
Piston area	0.93	0.87–0.96
Tonsillar descent area	0.96	0.92–0.98

ICC = intraclass correlation coefficients; Average ICC value above 0.70 signifies a strong agreement between independent raters; PCF = posterior cranial fossa.

absolute agreement. The average ICC value was >0.70 for each measure (Table 2), signifying strong agreement between the 2 independent raters.

2.4. Statistical analysis

All statistical analyses were performed using SPSS 23 (SPSS Inc., Chicago, IL) and Excel 2010 (Microsoft, Redmond, WA). The demographic characteristics, comorbidities, and preoperative symptoms of the improved and unimproved groups were compared, followed by a comparison of the morphological data for the 2 groups. Bivariate data were compared using Pearson chi-square test. In terms of continuous variables, the distributions of the improved and unimproved groups were tested separately using the Shapiro–Wilk method to determine normality; this was followed by Levene's equality of variances test to gauge the similarity of the data distributions. An independent-samples *t* test was performed if the data of the 2 groups were normally distributed and their variances were equal. Otherwise, the data were analyzed using the Mann–Whitney *U* test. The statistical results for continuous variables were recorded as means \pm SD, median (IQR), or median (range) according to the data distribution. All tests were 2-tailed, and a *P* value $<.05$ was considered to indicate statistical significance.

3. Results

Of the 39 patients who underwent PFD, 24 (61.5%) showed improvement and 15 (38.5%) showed no improvement after surgery. Table 3 lists the demographic characteristics, preoperative comorbidities, and preoperative symptoms of the 2 groups.

Table 3**Demographic characteristics, preoperative symptoms, and comorbidities of patients in the improved and unimproved groups.**

	Improved group (n=24)	Unimproved group (n=15)	<i>P</i> value
Basic information			
Sex (male/female)	6/18	4/11	.91
Age (years), mean \pm SD	49.7 \pm 9.9	45.9 \pm 9.4	.24
Duration of symptoms (months), median (IQR)	30 (107)	12 (66)	.65
Duration of follow-up (months), median (IQR)	26 (29)	34 (39)	.65
Comorbidity			
Syringomyelia	21	14	.56
Scoliosis	4	2	.78
Hydrocephalus	3	0	.15
Preoperative symptom			
Headache	7	4	.87
Neck pain	3	1	.56
Shoulder pain	1	2	.30
back pain	2	2	.62
upper limb pain	6	5	.57
lower limb pain	2	0	.25
Dizziness	3	0	.27
Upper limb numbness	14	14	.02
Upper limb weakness	7	10	.02
Muscular atrophy	2	0	.25
Lower limb numbness	4	5	.23
Lower limb weakness	4	4	.45
Gait instability	2	2	.62

IQR = interquartile range, SD = standard deviation.

The 18 females and 6 males in the improved group had a mean age of 49.7 ± 9.9 years. The mean age of the 11 females and 4 males in the unimproved group was 45.9 ± 9.4 years. There was no statistically significant difference in the sex ($P=.91$) or age ($P=.24$) distributions of the 2 groups. The median durations of preoperative symptoms were 30 months and 12 months ($P=.65$) and the median follow-up durations were 26 and 24 months ($P=.65$) in the improved group and unimproved group, respectively. Of the 24 patients in the improved group, 21 had syringomyelia, 4 had scoliosis, and 3 had hydrocephalus. Of the 15 patients in the unimproved group, 14 had syringomyelia, 2 had scoliosis, and none had hydrocephalus. There were no differences between the groups regarding preoperative comorbidities, indicating that the latter were unlikely to have influenced the outcomes after PFD. According to the pain location, preoperative pain occurred as headache, neck pain, shoulder pain, back pain, upper limb pain, and lower limb pain. There were no significant differences in the preoperative pain symptoms of the 2 groups. Of the patients with preoperative non-pain symptoms, patients in the unimproved were more likely than improved patients to exhibit numbness (odds ratio [OR]=10, $P=.02$) or muscle weakness (OR=4.86, $P=.02$) in the upper limbs. Upper limb numbness was reported by 14 (58%) of the 24 patients in the improved group and 14 (93%) of the 15 patients in the unimproved group. Upper limb weakness was reported by 7 (29%) patients in the improved group and 10 (67%) in the unimproved group. The differences between the groups in lower limb numbness, lower limb weakness, muscular atrophy, dizziness, and gait instability were not significant. Table 4 summarizes the statistical results of the 13 liner parameters, 8

Table 4
Comparison of improved and unimproved groups with respect to the parameters measured on the magnetic resonance images.

	Improved group		Unimproved group		P value
	n	Mean ± SD	n	Mean ± SD	
Liner parameters					
Clivus (mm)	24	40.3 ± 3.4	15	41 ± 2.9	.53
McRae line (mm)	24	34.3 ± 3.3	15	33.4 ± 2.6	.35
Supraocciput (mm)	24	39 ± 4.9	15	39.1 ± 5.5	.96
Tentorium (mm)	7	50 ± 5.1	7	45.5 ± 2.5	.06
Tentorium-clivus line (mm)	7	56.2 ± 5.8	7	57.9 ± 6.7	.63
PCF deep (mm)	24	32.6 ± 3.8	15	31.8 ± 4.8	.54
PCF height (mm)	7	62.3 ± 5	7	58.4 ± 3.5	.12
Twining line (mm)	24	84.2 ± 5	15	84.4 ± 4.2	.86
Tonsillar descent (mm)	24	11 ± 4	15	11.9 ± 5.7	.54
Tonsillar width (mm)	24	14.8 ± 2.4	15	14.8 ± 2.8	.98
Pons height (mm)	24	35.3 ± 6.4	15	34.8 ± 3.3	.75
Fastigium height (mm)	24	26.5 ± 2.9	15	26.5 ± 4.1	.99
Syrinx size (mm)	21	9.2 ± 2.9	14	9.5 ± 2.5	.73
Angular parameters					
Clival angle (°)	24	54.5 ± 6.6	15	52.1 ± 7.2	.30
Supraoccipital angle (°)	24	46.8 ± 10.3	15	48.3 ± 9.1	.65
Tentorial angle (°)	12	41.1 ± 6.3	10	41.5 ± 5.4	.87
Tentorial-supraoccipital (°)	12	88.6 ± 9.3	10	94.7 ± 10.4	.16
Twining-supraoccipital angle (°)	24	48.3 ± 6.4	15	47.8 ± 6.7	.50
Basal angle (°)	24	133.2 ± 6.4	15	135 ± 6.1	.38
Cervicomedullary angle (°)	24	154.4 ± 8.9	15	153.9 ± 8.7	.89
Wackenheim angle (°)	24	151.5 ± 9.7	15	148.3 ± 6.3	.25
Areal parameters					
PCF osseous area (cm ²)	24	17.9 ± 2.4	15	17.6 ± 2.2	.69
PCF area (cm ²)	7	31.7 ± 3.2	7	29.1 ± 2.2	.11
Tonsillar descent area (cm ²)	24	0.84 ± 0.41	15	0.94 ± 0.61	.53
Piston area (cm ²)	24	1.90 ± 0.78	15	2.02 ± 1.08	.68
Relative ratios					
PCF deep / the length of Twining line	24	2.6 ± 0.3	15	2.7 ± 0.45	.38
PCF height / the length of Twining line	7	0.74 ± 0.07	7	0.71 ± 0.06	.34
PCF osseous area / tonsillar descent area	24	26.2 ± 13.7	15	26.9 ± 16.3	.89
PCF osseous area / piston area	24	10.9 ± 4.8	15	11.1 ± 5.4	.88

SD = standard deviation, PCF = posterior cranial fossa.

angular parameters, 4 areal parameters, and 4 relative ratios evaluated in this study. Contrary to our expectations, there were no significant differences in the PCF morphology of the improved and unimproved groups.

4. Discussion

The pathogenesis of CMI is unclear, but it has been attributed to an anterior cephalic mesodermal defect that occurs during embryonic development and contributes to occipital bone hypoplasia, resulting in a reduction of PCF volume. Brain structures, such as the cerebellum, continue to develop normally, but the narrow PCF cannot accommodate them, leading to the herniation of the cerebellar tonsil into the spinal canal and the obstruction of CSF flow. These pathological changes damage the cerebellum, brainstem, spinal cord, lower cranial nerves, and upper cervical nerves, leading to clinical symptoms of pain, sensory or motor dysfunction, muscle atrophy, and, eventually, ataxia.^[21] After nearly 70 years of technical development, PFD is now widely used in the treatment of CMI.^[22] By partly removing the bony structures of the occiput and posterior atlas, PFD reconstructs the subdural environment and increases the volume of the PCF and cervical spinal canal, which relieves the compression of nerve structures in the narrow PCF and improves

CSF flow in the craniocervical junction.^[7] The postoperative improvement rates reported in the literature vary widely, ranging from 46% to 89%,^[3,6,23–28] most likely reflecting differences in inclusion criteria, surgical effect assessment, operation type, and follow-up time. The postoperative improvement rate in our series was 61.5%. Although the symptoms of a majority of patients improved or disappeared, there were still some patients whose symptoms were unchanged or had even worsened. This lack of a positive outcome after PFD was likely the result of poor patient selection. If not all patients with CMI will benefit from PFD, a method to preoperatively predict the surgical outcome is needed.^[8]

In 2015, Greenberg et al developed the Chiari Severity Index, based on the clinical manifestations and imaging features of CMI, to predict the efficacy of PFD. The presence of myelopathic symptoms, such as numbness, weakness, hyperreflexia, or unsteady gait, predicted a worse outcome.^[29] In their study of the relationship between preoperative symptoms and surgical effect, Hekman et al applied the CCOS scale to 167 patients with CMI and demonstrated that sensory deficits correlated with poor outcomes after PFD.^[10] This result is consistent with our own findings. In our patients, the myelopathic symptoms were further subdivided into upper limb numbness, upper limb weakness, lower limb numbness, lower limb weakness, and muscle atrophy.

Upper limb numbness and upper limb weakness were identified as unfavorable factors affecting the efficacy of PFD. The improvement rates of patients with postoperative upper limb numbness and upper limb weakness were 50% and 41%, respectively. Limb numbness and weakness are common symptoms of syringomyelia, but the relationship between preoperative syringomyelia and surgical outcome is controversial. Greenberg's study determined a lower improvement rate in patients with a syrinx >6 mm (55% vs 74% in those with a syrinx <6 mm). The authors suggested that a larger syrinx represents more serious spinal cord injury and, therefore, the more likely persistence of related symptoms. However, Hekman et al reported a postoperative improvement rate that was 3.94 times higher in patients with than without syringomyelia. In a retrospective study, Kalb evaluated 104 patients with CMI who underwent PFD. Patients with syringomyelia had a slightly lower rate of improvement in headache and sensorimotor dysfunction (62% vs 73%), but the authors found no relationship between symptom deterioration and syringomyelia.^[30] In our patients, neither the presence of syringomyelia nor preoperative syrinx size influenced the surgical outcome after PFD, perhaps because CMI often causes the formation of non-communicating syringes. The dilated central canal exhibits a propensity to dissect into the spinal cord parenchyma and even to extend through the pial surface to communicate with the subarachnoid space. The CSF in the damaged central canal flows out along the pressure gradient, causing the collapse of the cavity wall. As seen on the MR images, the syrinx shrinks or even disappears completely.^[30,31] The rates of syrinx reduction range from 44% to 100%.^[3] Batztorf et al retrospectively analyzed the medical records of 177 adult patients with Chiari malformation and concluded that postoperative symptomatic improvement related to syringomyelia was associated with a reduction in syrinx cavity size.^[12] However, other researchers found no correlation between postoperative clinical condition and syrinx size.^[24] This discrepancy might be due to the fact that the symptoms of syringomyelia are related primarily to the degree of injury to the spinal cord parenchyma. By contrast, because of spontaneous drainage between the syrinx cavity and the subarachnoid space, the syrinx size is not proportional to the degree of spinal cord injury. In patients with irreversible structural damage to the spinal cord due to preoperative syringomyelia, the resulting neurological dysfunction will persist even if the syrinx shrinks after surgery.^[32]

Despite our analysis of a relatively large number of morphological parameters of PCF, including lines, angles, areas, and relative ratios, we were unable to distinguish any radiological factors predictive of surgical outcome. In 2016, Alperin et al conducted a prospective study using preoperative MR images to predict the short-term outcomes of CMI patients. Several morphometric parameters were similar to those evaluated in the current study, including tonsillar herniation, clivus length, supraocciput length, and clivoaxial angle, but these authors were also unable to identify predictive morphological factors and considered physiological measures to be stronger predictors than morphological measures.^[8] Utilizing cine phase-contrast MR imaging (a dynamic MR technique) prior to surgery, Alperin et al found that preoperative maximal cord displacement in the upper cervical region and intracranial volume change (ICVC) during a cardiac cycle were predictors of decompression outcome in patients with CMI. During the systolic phase, intracranial pressure (ICP) increases rapidly because arterial blood flows increasingly into the skull while the amount of intracranial CSF entering the spinal canal is insufficient. The cerebellum, medulla

oblongata, and upper cervical cord move downward to accommodate the increased ICP. The greater maximal displacement of the upper cervical cord indirectly reflects the greater fluctuation of ICP in a cardiac cycle as well as the larger degree of CSF-flow obstruction at the foramen magnum. Regarding the ICVC, a smaller change implies that the cranial cavity is too small to accommodate the normal fluctuation in intracranial blood volume and CSF volume along with the beating heart. Patients with greater maximal upper cervical cord displacement and a lower ICVC during the cardiac cycle are more likely to respond favorably to PFD that appropriately increases PCF volume, enlarges the buffer space against an ICP fluctuation, and resolves the impairment of CSF flow.^[6,8,33] Another study used cine phase-contrast MR imaging to directly analyze the relationship between preoperative CSF flow dynamics and the efficacy of PFD. The authors concluded that patients with obstructed hindbrain CSF flow respond better to decompression than do patients with a normal CSF flow. The degree of hindbrain CSF flow obstruction was associated with preoperative symptoms and may thus be relevant in predicting the surgical response.^[6] The study's authors also speculated that symptoms in patients with normal hindbrain CSF flow are multifactorial in origin.

Although the standard for the diagnosis of CMI is a cerebellar tonsil that descends >5 mm below the foramen magnum, the degree of tonsillar descent was shown to be a poor sole predictor of the development of symptoms,^[2,34] as many asymptomatic patients have a low cerebellar tonsil position, and symptomatic patients may have a normally positioned tonsil. Several studies have also demonstrated that the degree of tonsillar descent does not influence the improvement in symptoms after PFD, which was also observed in our study.^[2,34]

In the absence of a 3-dimensional reconstruction protocol during preoperative MRI, we could not calculate the exact volume of the PCF. Furthermore, the calculation is complicated and often requires professional software, which limits its clinical application. The volumes of different structures in the skull cavity, including the intracranial volume, PCF volume, supratentorial volume, herniated volume, 4th ventricle volume, and hindbrain volume, have been measured,^[4,5,8] but the volumetric measurements failed to predict the response of CMI patients to PFD. As the brain tissue on either side of the median sagittal plane approximates a mirror-symmetric distribution, relevant areas in the median sagittal plane of the PCF are commonly used as morphological parameters.^[17-19] We measured the PCF area, PCF osseous area, tonsillar descent area, and piston area in our study, but none of these morphological indicators was predictive of improvement after PFD. This was probably because the main pathogenesis of CMI is the mismatch between the dysplastic PCF and the normally developed hindbrain, the degree of which depends on the skeletal anatomy of the individual patient. Moreover, sex, ethnic background, or body mass index may interfere with measurements of the PCF and intracranial volume.^[17] A study with a small sample concluded that the response to PFD correlated positively with the magnitude of the increase in PCF volume after surgery.^[5] Symptoms related to CMI were completely relieved, without complications, when the PCF volume increased by 15%. A pediatric study of CMI found that an increase in the postoperative PCF volume, especially the volume of the cisterna magna, was associated with a greater likelihood of headache resolution.^[13] It also confirmed the important role of CSF flow disturbances in the pathology of CMI. Our study likewise failed to identify radiological predictive

factors based on preoperative conventional MRI. Unlike cine phase-contrast MR imaging, conventional MR imaging, cannot display either CSF flow dynamics or indirect indicators thereof, such as maximal displacement of the upper cervical cord.

The present study had several limitations. First, because it was a retrospective analysis, there was no unified study protocol established before the study. Second, some patients were excluded due to lack of preoperative MR imaging data, which very likely caused selection bias. Although we strived to obtain preoperative clinical information from the hospital medical records and follow-up records, the lack of a unified CMI-related symptom questionnaire at admission may have resulted in the omission from the patient history of minor symptoms that did not cause obvious discomfort. Additionally, only cranial-cervical MR imaging examinations were preoperatively performed in most patients in our cohort, which prevented measurements of the size and length of the syrinx in the thoracolumbar region. Moreover, none of the patients with CMI underwent preoperative computed tomography, which would have displayed the bony structure more accurately than MR imaging. To ensure the homogeneity of the included patients, strict inclusion and exclusion criteria were formulated. However, after the elimination of patients who did not meet our criteria and those who were lost to follow up, the sample size was relatively small, which limited the study's statistical power. Future prospective large-sample studies will overcome most of the above limitations.

5. Conclusion

Patients with CMI who present with preoperative upper limb numbness or upper limb weakness are less likely to improve after PFD. PCF morphology is not predictive of the outcome of therapeutic surgical decompression. Instead, pathophysiological factors, such as irreversible structural damage of the spinal cord parenchyma and impairment of the CSF flow in the craniocervical junction, seem to be of greater predictive value.

Author contributions

Conceptualization: Zheng Liu, Meihua Li.

Data curation: Zheng Liu, Zheng Hao.

Formal analysis: Zheng Liu, Si Hu, Yeyu Zhao.

Funding acquisition: Meihua Li.

Investigation: Meihua Li.

Methodology: Zheng Liu, Yeyu Zhao.

Project administration: Meihua Li.

Resources: Meihua Li.

Software: Zheng Liu, Si Hu.

Supervision: Meihua Li.

Writing – original draft: Zheng Liu.

Writing – review & editing: Zheng Hao, Si Hu, Yeyu Zhao, Meihua Li.

References

- Beschachio DA, Khaleel Z, Shah LM. Odontoid process inclination in normal adults and in an adult population with Chiari malformation Type I. *J Neurosurg Spine* 2015;23:701–6.
- Khalsa SSS, Geh N, Martin BA, et al. Morphometric and volumetric comparison of 102 children with symptomatic and asymptomatic Chiari malformation Type I. *J Neurosurg Pediatr* 2018;21:65–71.
- Attenello FJ, McGirt MJ, Gathinji M, et al. Outcome of Chiari-associated syringomyelia after hindbrain decompression in children: analysis of 49 consecutive cases. *Neurosurgery* 2008;62:1307–13.
- Grangeon L, Puy L, Gilard V, et al. Predictive factors of headache resolution after Chiari Type 1 malformation surgery. *World Neurosurg* 2018;110:e60–6.
- Noudel R, Gomis P, Sotoares G, et al. Posterior fossa volume increase after surgery for Chiari malformation Type I: a quantitative assessment using magnetic resonance imaging and correlations with the treatment response. *J Neurosurg* 2011;115:647–58.
- McGirt MJ, Nimjee SM, Fuchs HE, et al. Relationship of cine phase-contrast magnetic resonance imaging with outcome after decompression for Chiari I malformations. *Neurosurgery* 2006;59:140–6.
- Zhao JL, Li MH, Wang CL, et al. A systematic review of Chiari I malformation: techniques and outcomes. *World Neurosurg* 2016; 88:7–14.
- Alperin N, Loftus JR, Bagci AM, et al. Magnetic resonance imaging-based measures predictive of short-term surgical outcome in patients with Chiari malformation Type I: a pilot study. *J Neurosurg Spine* 2017;26:28–38.
- McGirt MJ, Attenello FJ, Atiba A, et al. Symptom recurrence after suboccipital decompression for pediatric Chiari I malformation: analysis of 256 consecutive cases. *Child's Nerv Syst* 2008;24:1333–9.
- Hekman KE, Aliaga L, Straus D, et al. Positive and negative predictors for good outcome after decompressive surgery for Chiari malformation type 1 as scored on the Chicago Chiari Outcome Scale. *Neurol Res* 2013;34:694–700.
- Sodhro AH, Malokani AS, Sodhro GH, et al. An adaptive QoS computation for medical data processing in intelligent healthcare applications. *Neural Comput Appl* 2019;23–31.
- Batzdorf U, McArthur DL, Bentson JR. Surgical treatment of Chiari malformation with and without syringomyelia: experience with 177 adult patients. *J Neurosurg* 2013;118:232–42.
- Khalsa SSS, Siu A, DeFreitas TA, et al. Comparison of posterior fossa volumes and clinical outcomes after decompression of Chiari malformation Type I. *J Neurosurg Pediatr* 2017;19:511–7.
- Aliaga L, Hekman KE, Yassari R, et al. A novel scoring system for assessing Chiari malformation type I treatment outcomes. *Neurosurgery* 2012;70:656–64.
- Greenberg JK, Milner E, Yarbrough CK, et al. Outcome methods used in clinical studies of Chiari malformation Type I: a systematic review. *J Neurosurg* 2015;122:262–72.
- Yarbrough CK, Greenberg JK, Smyth MD, et al. External validation of the Chicago Chiari Outcome Scale. *J Neurosurg Pediatr* 2014;13: 679–84.
- Houston JR, Eppelheimer MS, Pahlavian SH, et al. A morphometric assessment of type I Chiari malformation above the McRae line: a retrospective case-control study in 302 adult female subjects. *J Neuro-radiol* 2018;45:23–31.
- Eppelheimer MS, Houston JR, Bapuraj JR, et al. A retrospective 2D morphometric analysis of adult female Chiari type I patients with commonly reported and related conditions. *Front Neuroanat* 2018;12.
- Urbizu A, Ferré A, Poca MA, et al. Cephalometric oropharynx and oral cavity analysis in Chiari malformation Type I: a retrospective case-control study. *J Neurosurg* 2017;126:626–33.
- Strahle J, Muraszko KM, Garton HJ, et al. Syrinx location and size according to etiology: identification of Chiari-associated syrinx. *J Neurosurg Pediatr* 2015;16:21–9.
- Noudel R, Jovenin N, Eap C, et al. Incidence of basioccipital hypoplasia in Chiari malformation type I: comparative morphometric study of the posterior cranial fossa. *Clinical article. J Neurosurg* 2009;111:1046–52.
- Klekamp J. Surgical treatment of Chiari I malformation—analysis of intraoperative findings, complications, and outcome for 371 foramen magnum decompressions. *Neurosurgery* 2012;71:365–80.
- Alzate JC, Kothbauer KF, Jallo GI, et al. Treatment of Chiari I malformation in patients with and without syringomyelia: a consecutive series of 66 cases. *Neurosurg Focus* 2001;11:1–9.
- Navarro R, Olavarria G, Seshadri R, et al. Surgical results of posterior fossa decompression for patients with Chiari I malformation. *Child's Nerv Syst* 2004;20:349–56.
- Dyste GN, Menezes AH, VanGilder JC. Symptomatic Chiari malformations. An analysis of presentation, management, and long-term outcome. *J Neurosurg* 1989;71:159–168.
- Parker SL, Godil SS, Zuckerman SL, et al. Comprehensive assessment of 1-year outcomes and determination of minimum clinically important difference in pain, disability, and quality of life after suboccipital decompression for Chiari malformation I in adults. *Neurosurgery* 2013;73:569–81.

- [27] Kalb S, Perez-Orribo L, Mahan M, et al. Evaluation of operative procedures for symptomatic outcome after decompression surgery for Chiari type I malformation. *J Clin Neurosci* 2012;19:1268–72.
- [28] Tisell M, Wallskog J, Linde M. Long-term outcome after surgery for Chiari I malformation. *Acta Neurol Scand* 2009;120:295–9.
- [29] Greenberg JK, Yarbrough CK, Radmanesh A, et al. The Chiari severity index: a preoperative grading system for Chiari malformation type 1. *Neurosurgery* 2015;76:279–85.
- [30] Bogdanov EI, Mendelevich EG. Syrinx size and duration of symptoms predict the pace of progressive myelopathy: retrospective analysis of 103 unoperated cases with craniocervical junction malformations and syringomyelia. *Clin Neurol Neurosurg* 2002;104:90–7.
- [31] Milhorat TH. Classification of syringomyelia. *Neurosurg Focus* 2000;8:E1.
- [32] Sakamoto H, Nishikawa M, Hakuba A, et al. Expansive suboccipital cranioplasty for the treatment of syringomyelia associated with Chiari malformation. *Acta Neurochir (Wien)* 1999;141:949–60.
- [33] Hofmann E, Warmuth-Metz M, Bendszus M, et al. Phase-contrast MR imaging of the cervical CSF and spinal cord: volumetric motion analysis in patients with Chiari I malformation. *AJNR Am J Neuroradiol* 2000;21:151–8.
- [34] Trigylidas T, Baronia B, Vassilyadi M, et al. Posterior fossa dimension and volume estimates in pediatric patients with Chiari I malformations. *Child's Nerv Syst* 2008;24:329–36.